

Supporting Information

Eder et al. 10.1073/pnas.1205653109

SI Text

Magnetic Field Settings. A magnetic cell in a suspension of cells has magnetorotational mobility, $\alpha = \mu/(2\pi\eta C)$ where μ is the permanent magnetic dipole moment of the cell, C is its hydrodynamic friction coefficient, and η is the viscosity of the liquid in which the cell is immersed. The population of magnetic cells in a dissociated tissue preparation is characterized by a distribution $n(\alpha)$ of magnetorotational mobility and we ask which fraction of the population can be set in rotational motion by an external magnetic field of intensity B and rotational frequency f_B . Because the critical frequency for rotation in synchrony with an external magnetic field is given by $f_B^{\max} = \alpha B$, the field (B, f_B) setting selects those cells in the population that meet the criterion:

$$\alpha \geq \frac{f_B}{B}. \quad [\text{S1}]$$

In other words, cells satisfying [S1] can be easily recognized by their rotational motion when scanning the preparation for rotating cells. These cells are termed “experimentally well accessible” and their key parameters (μ, a) plot on the upper left in the rotational actuation nomogram (Fig. S1). If the frequency f_B is slightly increased beyond the critical frequency f_B^{\max} of a given cell, then that cell stops rotating in synchrony with the field and starts to make clockwise and anticlockwise quarter-turns in rapidly alternating sequence. This phenomenon is equivalent to apparently chaotic swimming trajectories displayed in magnetic bacteria when the driving frequency exceeds the critical frequency (1). With yet larger excess frequency, the amplitude of the oscillatory motion decreases fast and eventually (say at $f_B/f_B^{\max} > 2$) is hardly recognizable, that is, the cell appears to shiver slightly, which makes it difficult to discriminate magnetic actuation against Brownian motion. Therefore, although potentially still accessible with the rotating field method, cells with $f_B^{\max} < f_B$ can in general not be considered experimentally well accessible, hence our cut-off criterion [S1]. It is obvious from [S1] that a slowly rotating but strong magnetic field increases the chances of identifying magnetic cells by their rotational motion when visually screening a dissociated tissue preparation. We found $f_B = 0.33$ Hz to be an experimentally convenient rotation frequency, which is a good compromise between search speed and probability of finding a spinning cell. By limiting the magnetic field intensity to values well below 5 mT (e.g., 2.1 mT, as in Fig. S1), one can avoid remagnetization of biogenic single-domain magnetite, in which case their original magnetic state would be irreversibly lost. This restriction is of course relevant only if the aim is to measure the natural remanent magnetic dipole moment of identified cells. If harvesting of magnetic cells is the key task instead, then the magnetic field intensity should be set to larger values. When going from 2.1 to 8.4 mT, cells with four times smaller magnetic dipole moment become theoretically accessible (for a given cell size), or for a given magnetic moment, cells with $4^{1/3} \approx 1.6$ times larger diameter. However, upon further increasing the field strength, one runs the risk of magnetizing cells containing higher amounts of biologically bound iron or waste, which need to be sorted out in a second stage process.

Ellipsoidal Cells. Elongated cells spinning about figure axis i are modeled using the frictional resistance coefficients C_i for the general ellipsoid, given by Jeffery (2),

$$C_i = \frac{16\pi}{3} \frac{a_j^2 + a_k^2}{a_j^2 P_j + a_k^2 P_k}, \quad [\text{S2}]$$

which depend on the geometry of the cell (semiaxes a_1, a_2, a_3), and the volume of the fluid in which the cell is immersed, through the upper limit s_{\max} of the elliptic integrals

$$P_\lambda = \int_0^{s_{\max}} \frac{ds}{(a_\lambda^2 + s) \sqrt{\prod_{v=1}^3 (a_v^2 + s)}}, \quad [\text{S3}]$$

where s is the algebraically largest root of the equation for an ellipsoidal surface in the liquid that is confocal with the immersed ellipsoidal cell,

$$\frac{x_1^2}{a_1^2 + s} + \frac{x_2^2}{a_2^2 + s} + \frac{x_3^2}{a_3^2 + s} = 1, \quad [\text{S4}]$$

where the surface of the cell is given by $s = 0$. The rotation of an ellipsoidal cell produces a flow field of ellipsoidal symmetry with radially outward decreasing angular velocity, that is, adjacent fluid layers (ellipsoidal shells) are rotated differentially. For a fluid boundary located at s_{\max} , the no-flow boundary condition implies enhanced shear stress (friction) so that the proximity of a fluid boundary to a rotating cell always increases C_i . This is mathematically obvious from Eq. S3, which has a monotonously decreasing, but always positive, finite kernel, so that increasing s_{\max} always increases the integral; because C_i has P_i in the denominator, C_i is minimum for $s_{\max} \rightarrow \infty$. In the limit $s_{\max} \rightarrow \infty$, P_i can be evaluated in terms of elliptic integrals of the first and second kind (3) and it is worth mentioning that P_i is mathematically equivalent to the demagnetization tensor of a homogeneously magnetized general ellipsoid (4, 5).

Estimation of Errors. Because the magnetic cells may be floating only tens of microns above the microscope slide, the assumption of a distant fluid boundary is almost certainly violated and we have to ask by how much we underestimate the true C when using the limit case expression for $s_{\max} \rightarrow \infty$. To begin with, we consider a cell of spherical geometry as this case can be treated algebraically. For a sphere with radius $a \equiv a_1 = a_2 = a_3$, expression S3 evaluates to

$$P(\sigma_{\max}) = \frac{1}{a^3} \int_0^{\sigma_{\max}} \frac{d\sigma}{(1 + \sigma)^{5/2}} = \frac{2}{3a^3} \left[1 - \frac{1}{(1 + \sigma_{\max})^{3/2}} \right], \quad [\text{S5}]$$

where $\sigma_{\max} = s_{\max}/a^2$. From Eq. S4 we can express b , the radius of the boundary shell related to the integration limit S_{\max} , in terms of σ_{\max} , i.e., $b^2 = a^2(1 + \sigma_{\max})$, and recast Eq. S5 into

$$P(a, b) = \frac{2}{3} \left(\frac{1}{a^3} - \frac{1}{b^3} \right). \quad [\text{S6}]$$

Putting [S6] into [S2], we finally have

$$C(b/a) = 8\pi \frac{a^3}{1 - (a/b)^3}. \quad [\text{S7}]$$

For $b \rightarrow \infty$, expression **S7** converges to $C_\infty = 8\pi a^3$, which is the rotational friction coefficient of an unbounded sphere. As can be seen in Fig. S2, $C(b/a)$ deviates from C_∞ , by less than 10% when the clear distance d between cell surface and fluid boundary exceeds 0.6 times the cell diameter. The deviation drops below the 1% level for $d/2a \geq 1.8$. The fast convergence of $C(b/a)$ towards C_∞ is mathematically intuitive from the $(1 - (a/b)^3)^{-1}$ dependency (see Eq. **S7**). Fig. S3 shows the proximity effect of a boundary layer on the rotational friction coefficient for a general ellipsoid with semiaxes $a_1 = 1.8$, $a_2 = 0.9$, $a_3 = 0.6$. For rotation about the long axis ($i = 1$), the coefficient $C_1(b/a_1)$ deviates by less than 10% from its limit value $C_{1,\infty}$ once the long axis of the fluid boundary is at $b > 1.42a_1$. For rotation about the short axis ($i = 3$), the relative deviation of $C_3(b/a_1)$ from $C_{3,\infty}$ is about twice as large at a given b/a_1 ratio compared to rotation about the short axis. This is due to the fact that rotation about a short axis means that the long axis is in the equatorial (rotation) plane and therefore is closer to the fluid boundary than the intermediate axis is during rotation about the long axis.

Because the estimated magnetic moment μ is proportional to C_i , a possible underestimation of the distance of the fluid boundary from the cell implies an underestimation of μ . Likewise, the viscosity measurement was done on the pure buffer solution before it was added to the suspension of cells, whereas debris from the dissociation procedure is likely to slightly enhance the actual viscosity of the fluid in which the isolated cells are immersed. Hence, both effects have the same tendency. Therefore, our estimates of μ are rather on the conservative side. The remaining source of error is the determination of the cell dimensions under the light microscope, which is diffraction limited. The optically determined uncertainty in the cell axis is estimated to be 0.5 μm in the focal plane and 1 μm in the focal depth, both of which are small compared to the typical cell dimensions of 10 μm .

Differential Rotation. This scenario applies to the case of a magnetic inclusion that is not mechanically coupled to the cell membrane but viscously suspended in the cytoplasm. When spinning at angular frequency ω_a due to a rotating external magnetic field, the magnetic inclusion transmits shear stress to the cell membrane through the viscosity of the cytoplasm. The shear stress in turn sets the cell membrane in rotation, albeit at a rate $\omega_b < \omega_a$. The differential rotation $\omega_a - \omega_b$ can be calculated algebraically for the geometrically simple case of a spherical inclusion of radius a , located in the center of a spherical cell membrane of radius b . The cell membrane now defines the fluid boundary for the inclusion so that the viscous resistance coefficient of the inclusion is given by Eq. **S7**. Since the fluid boundary rotates at rate ω_b , the couple acting on the inclusion by the fluid volume within $a < r < b$ is given by

$$N_a = -8\pi\eta_{cp} \frac{a^3 b^3}{b^3 - a^3} (\omega_a - \omega_b), \quad [\text{S8}]$$

where η_{cp} is the viscosity of the cytoplasm. The couple acting on the rotating cell membrane by the external fluid of viscosity η is

$$N_b = -8\pi\eta b^3 \omega_b, \quad [\text{S9}]$$

and conversely, the couple needed to produce rotational motion of the cell membrane is $-N_b$, which is provided by the rotational motion of the inner fluid. By balancing the couples, we obtain the rotation rate of the cell relative to that of the inclusion as

$$\frac{\omega_b}{\omega_a} = \frac{\eta_{cp}/\eta}{\eta_{cp}/\eta + (b/a)^3 - 1}. \quad [\text{S10}]$$

The viscosity contrast η_{cp}/η can be regarded as coupling strength. As seen in Fig. S4, a cell membrane of diameter 10 μm enclosing a 1 μm sized magnetic inclusion ($b/a = 10$) rotates at a distinctly lower rate than the inclusion does, even for a viscosity contrast as high as 100.

Induced Magnetization. A cell may have also induced magnetization in addition to remanent magnetization, in which case its magnetic susceptibility must be anisotropic in order for the external magnetic field to produce a torque on the induced magnetization. The torque due to anisotropic magnetic susceptibility is given by

$$N_{\text{ind}} = \frac{1}{2} \Delta\chi B^2 V \sin 2\psi \quad [\text{S11}]$$

(in c.g.s., e.g., 6), where V is the volume containing the anisotropic induced magnetization and $\Delta\chi$ is the difference in magnetic susceptibility between maximum and minimum axis of the susceptibility tensor. Incorporation of expression **S11** into the torque balance (c.f. Eq. 2 in main text), yields the following expression

$$\frac{\mu B}{2\pi\eta C} \sin \psi + \frac{1}{2} \frac{\Delta\chi B^2 V}{2\pi\eta C} \sin 2(\psi - \delta) = f_B, \quad [\text{S12}]$$

where δ is the orientation of the axis of maximum susceptibility relative to the remanent magnetization axis, with δ reckoned positive from the remanent magnetic vector toward the (counterclockwise rotating) magnetic field vector. Introducing $f_{\text{rem}}^{\text{max}}$ and $f_{\text{ind}}^{\text{max}}$ as the critical frequency for the case of remanent-only or induced-only magnetization, respectively, Eq. **S12** can be rewritten as

$$f_{\text{rem}}^{\text{max}} \sin \psi + f_{\text{ind}}^{\text{max}} \sin 2(\psi - \delta) = f_B. \quad [\text{S13}]$$

Maximization of Eq. **S13** yields $f_B^{\text{max}}(\rho; \delta)$, the maximum frequency of the external field up to which the cell can rotate synchronously with the field, where $\rho = f_{\text{ind}}^{\text{max}}/f_{\text{rem}}^{\text{max}}$. Mathematically speaking, the two most important solutions to Eq. **S13** occur for $\delta = \pm\pi/4$:

- i. $\delta = +\pi/4$, i.e., induced and remanent torque add up coherently at any field strength:

$$f_B^{\text{max}} = f_{\text{rem}}^{\text{max}} + f_{\text{ind}}^{\text{max}}. \quad [\text{S14}]$$

- ii. $\delta = -\pi/4$, i.e., the remanent torque opposes the induced torque:

$$\frac{f_B^{\text{max}}}{f_{\text{rem}}^{\text{max}}} = \begin{cases} 1 - \rho & \text{for } \rho \leq \frac{1}{4} \\ \frac{1}{4\rho} + \rho \sin \left[2 \left(\frac{\pi}{4} + \arcsin \frac{1}{4\rho} \right) \right] & \text{for } \rho > \frac{1}{4} \end{cases}, \quad [\text{S15}]$$

and the solution has the asymptote $f_B^{\text{max}} = f_{\text{ind}}^{\text{max}}$ (see also Fig. S5).

All other solutions fall between these two boundary lines (see Figs. S5 and S6).

Specifically for $\delta = \pm\pi/2$ and $\delta = 0$, the solution is:

$$\frac{f_B^{\text{max}}}{f_{\text{rem}}^{\text{max}}} = \sqrt{1 - \alpha^2} (1 + 2\alpha\rho) \quad \text{with } \alpha = \frac{-1\sqrt{1 + 32\rho^2}}{8\rho}.$$

Importantly, all solutions have unit slope for large values of ρ , so that $f_B^{\text{max}}(\rho \gg 1) \propto B^2$, that is, the maximum frequency increases quadratically with applied field intensity B .

Finally, the case $\delta = \pi/2$ deserves closer examination. Consider a magnetic inclusion whose dipole is dominated by magnetic

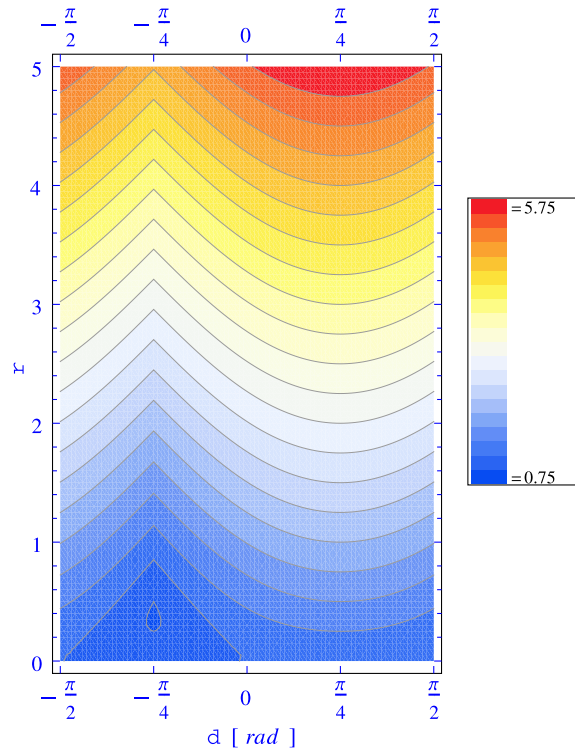


Fig. S6. Maximum frequency $f_B^{\max}(\rho; \delta) / f_{\text{rem}}^{\max}$ as a function of both induced-to-remanent ratio $\rho = f_{\text{ind}}^{\max} / f_{\text{rem}}^{\max}$ and angle δ .

